that fibronectin may play critical roles in lung cancer metastasis.[36] In this study, statistically significant overexpression of fibronectin was detected in the solid subtype of adenocarcinomas, although the expression in almost all of the adenocarcinomas was negative or weak. Vimentin is a structural protein from cells of mesenchymal origin.[37] Its expression level is higher in migratory epithelial cells and may contribute to the migratory and invasive phenotype of metastatic cells.[38] Significant correlations between high vimentin tumor cell expression and poor prognosis have previously been reported in both cases of hepatocellular carcinoma and lung cancer.[15,39] Vimentin and fibronectin have also been shown to contribute to EMT. EMT has been recognized as a characteristic of tumor cells invading the surrounding stroma. The characteristics of the EMT phenotype have been explained as being related to down-regulation of E-cadherin and up-regulation of vimentin or increased ZEB-1 expression.[40–42] The results of this study showed no significant difference in the E-cadherin or ZEB-1 expression among the tumor subtypes. Therefore, our current results do not suggest that the solid component in adenocarcinomas displayed the typical EMT phenotype.

In conclusion, our data showed that patients with pulmonary adenocarcinoma showing predominance of the solid component showed poorer outcomes than those with predominance of other nonsolid components. This study also showed high expression of laminin-5 in the solid component and suggested that this molecule may therefore play an important role in tumor progression of lung adenocarcinoma. Clarification of the molecular pathogenesis of the solid component in lung adenocarcinomas will be important in the future, which may be expected to contribute not only to individual patient care, but also to better selection and stratification for clinical trials and molecular studies.

REFERENCES

1. Asamura H, Goya T, Koshiishi Y, et al. A Japanese Lung Cancer Registry study: prognosis of 13,010 resected lung cancers. *J Thorac Oncol.* 2008;3:46–52.
2. Travis WD, Brambilla E, Noguchi M, et al. International association for the study of lung cancer/American Thoracic Society/European Respiratory Society: international multidisciplinary classification of lung adenocarcinoma: executive summary. *Proc Am Thorac Soc.* 2011;8:381–5.
3. Travis WD, Brambilla E, Noguchi M, et al. International Association for the Study of Lung Cancer/American Thoracic Society/European Respiratory Society international multidisciplinary classification of lung adenocarcinoma. *J Thorac Oncol.* 2011;6:244–85.
4. Travis WD, Brambilla E, Van Schil P, et al. Paradigm shifts in lung cancer as defined in the new IASLC/ATS/ERS lung adenocarcinoma classification. *Eur Respir J.* 2011;38:239–43.
5. Travis W, Brambilla E, Muller-Hermelink H, Harris C. World Health Organization classification of tumors. Pathology and genetics of the lung, pleura, thymus and heart. IARC Press; 2004.
6. Sica G, Yoshizawa A, Sima CS, et al. A grading system of lung adenocarcinomas based on histologic pattern is predictive of disease recurrence in stage I tumors. *Am J Surg Pathol.* 2010;34:1155–62.
7. Borczuk AC, Qian F, Kazeros A, et al. Invasive size is an independent predictor of survival in pulmonary adenocarcinoma. *Am J Surg Pathol.* 2009;33:462–9.
8. Noguchi M, Morikawa A, Kawasaki M, et al. Small adenocarcinoma of the lung. Histologic characteristics and prognosis. *Cancer.* 1995;75:2844–52.
9. Sakurai H, Maeshima A, Watanabe S, et al. Grade of stromal invasion in small adenocarcinoma of the lung: histopathological minimal invasion and prognosis. *Am J Surg Pathol.* 2004;28:198–206.
10. Yim J, Zhu LC, Chiriboga L, et al. Histologic features are important prognostic indicators in early stages lung adenocarcinomas. *Mod Pathol.* 2007;20:233–41.
11. Barletta JA, Yeap BY, Chirieac LR. Prognostic significance of grading in lung adenocarcinoma. *Cancer.* 2010;116:659–69.
12. Ohtaki Y, Yoshida J, Ishii G, et al. Prognostic significance of a solid component in pulmonary adenocarcinoma. *Ann Thorac Surg.* 2011;91:1051–7.
13. Petersen I, Kotb WF, Friedrich KH, et al. Core classification of lung cancer: correlating nuclear size and mitoses with ploidy and clinicopathological parameters. *Lung Cancer.* 2009;65:312–8.
14. Riquet M, Foucault C, Berna P, et al. Prognostic value of histology in resected lung cancer with emphasis on the relevance of the adenocarcinoma subtyping. *Ann Thorac Surg.* 2006;81:1988–95.
15. Al-Saad S, Al-Shibli K, Donnem T, et al. The prognostic impact of NF-kappaB p105, vimentin, E-cadherin and Par6 expression in epithelial and stromal compartment in non-small-cell lung cancer. *Br J Cancer.* 2008;99:1476–83.
16. Moriya Y, Niki T, Yamada T, et al. Increased expression of laminin-5 and its prognostic significance in lung adenocarcinomas of small size. An immunohistochemical analysis of 102 cases. *Cancer.* 2001;91:1129–41.
17. Sholl LM, Barletta JA, Yeap BY, et al. Sox2 protein expression is an independent poor prognostic indicator in stage I lung adenocarcinoma. *Am J Surg Pathol.* 2010;34:1193–8.
18. Motoi N, Szoke J, Riely GJ, et al. Lung adenocarcinoma: modification of the 2004 WHO mixed subtype to include the major histologic subtype suggests correlations between papillary and micropapillary adenocarcinoma subtypes, EGFR mutations and gene expression analysis. *Am J Surg Pathol.* 2008;32:810–27.
19. Sobin L, Wittekind C. TNM classification of malignant tumors. New York: Wiley and Sons; 2002.
20. Tsuta K, Ishii G, Nitadori J, et al. Comparison of the immunophenotypes of signet-ring cell carcinoma, solid adenocarcinoma with mucin production, and mucinous bronchioloalveolar carcinoma of the lung characterized by the presence of cytoplasmic mucin. *J Pathol.* 2006;209:78–87.
21. Hsu FD, Nielsen TO, Alkushi A, et al. Tissue microarrays are an effective quality assurance tool for diagnostic immunohistochemistry. *Mod Pathol.* 2002;15:1374–80.
22. Bryant CM, Albertus DL, Kim S, et al. Clinically relevant characterization of lung adenocarcinoma subtypes based on cellular pathways: an international validation study. *PLoS One.* 2010;5:e11712.
23. Eren B, Sar M, Oz B, Dincbas FH. MMP-2, TIMP-2 and CD44v6 expression in non-small-cell lung carcinomas. *Ann Acad Med Singapore.* 2008;37:32–9.
24. Maatta M, Soini Y, Paakko P, et al. Expression of the laminin gamma2 chain in different histological types of lung carcinoma. A study by immunohistochemistry and in situ hybridization. *J Pathol.* 1999;188:361–8.

25. Tsutsumida H, Nomoto M, Goto M, et al. A micropapillary pattern is predictive of a poor prognosis in lung adenocarcinoma, and reduced surfactant apoprotein A expression in the micropapillary pattern is an excellent indicator of a poor prognosis. *Mod Pathol.* 2007;20:638–47.
26. Yun J, Son CH, Um SJ, et al. A different TRAP220 expression in distinct histologic subtypes of lung adenocarcinoma and the prognostic significance. *Lung Cancer.* 2011;71:312–8.
27. Takatsuki H, Komatsu S, Sano R, et al. Adhesion of gastric carcinoma cells to peritoneum mediated by alpha3beta1 integrin (VLA-3). *Cancer Res.* 2004;64:6065–70.
28. Koshikawa N, Moriyama K, Takamura H, et al. Overexpression of laminin gamma2 chain monomer in invading gastric carcinoma cells. *Cancer Res.* 1999;59:5596–601.
29. Kosmehl H, Berndt A, Strassburger S, et al. Distribution of laminin and fibronectin isoforms in oral mucosa and oral squamous cell carcinoma. *Br J Cancer.* 1999;81:1071–9.
30. Pyke C, Romer J, Kallunki P, et al. The gamma 2 chain of kalinin/laminin 5 is preferentially expressed in invading malignant cells in human cancers. *Am J Pathol.* 1994;145:782–91.
31. Soini Y, Maatta M, Salo S, et al. Expression of the laminin gamma 2 chain in pancreatic adenocarcinoma. *J Pathol.* 1996;180: 290–4.
32. Yamaguchi Y, Ishii G, Kojima M, et al. Histopathologic features of the tumor budding in adenocarcinoma of the lung: tumor budding as an index to predict the potential aggressiveness. *J Thorac Oncol.* 2010;5:1361–8.
33. Salo S, Boutaud A, Hansen AJ, et al. Antibodies blocking adhesion and matrix binding domains of laminin-332 inhibit tumor growth and metastasis in vivo. *Int J Cancer.* 2009;125:1814–25.
34. Sawai H, Okada Y, Funahashi H, et al. Activation of focal adhesion kinase enhances the adhesion and invasion of pancreatic cancer cells via extracellular signal–regulated kinase-1/2 signaling pathway activation. *Mol Cancer.* 2005;4:37.
35. Shibata K, Kikkawa F, Nawa A, et al. Both focal adhesion kinase and c-Ras are required for the enhanced matrix metalloproteinase 9 secretion by fibronectin in ovarian cancer cells. *Cancer Res.* 1998;58:900–3.
36. Meng XN, Jin Y, Yu Y, et al. Characterisation of fibronectin-mediated FAK signalling pathways in lung cancer cell migration and invasion. *Br J Cancer.* 2009;101:327–34.
37. Leader M, Collins M, Patel J, Henry K. Vimentin: an evaluation of its role as a tumour marker. *Histopathology.* 1987;11:63–72.
38. Bindels S, Mestdagt M, Vandewalle C, et al. Regulation of vimentin by SIP1 in human epithelial breast tumor cells. *Oncogene.* 2006;25:4975–85.
39. Hu L, Lau SH, Tzang CH, et al. Association of Vimentin overexpression and hepatocellular carcinoma metastasis. *Oncogene.* 2004;23:298–302.
40. Takeyama Y, Sato M, Horio M, et al. Knockdown of ZEB1, a master epithelial-to-mesenchymal transition (EMT) gene, suppresses anchorage-independent cell growth of lung cancer cells. *Cancer Lett.* 2010;296:216–24.
41. Nieto MA. Epithelial–mesenchymal transitions in development and disease: old views and new perspectives. *Int J Dev Biol.* 2009;53:1541–7.
42. Voulgari A, Pintzas A. Epithelial–mesenchymal transition in cancer metastasis: mechanisms, markers and strategies to overcome drug resistance in the clinic. *Biochim Biophys Acta.* 2009; 1796:75–90.

Ann Surg Oncol (2012) 19:3953–3962
DOI 10.1245/s10434-012-2421-4

Annals of
SURGICAL ONCOLOGY
OFFICIAL JOURNAL OF THE SOCIETY OF SURGICAL ONCOLOGY

ORIGINAL ARTICLE – THORACIC ONCOLOGY

Recruitment of Podoplanin Positive Cancer-Associated Fibroblasts in Metastatic Lymph Nodes Predicts Poor Prognosis in Pathological N2 Stage III Lung Adenocarcinoma

Shinya Neri[1,2], Genichiro Ishii[1], Tetsuhiko Taira[1,2], Tomoyuki Hishida[2], Junji Yoshida[2], Mitsuyo Nishimura[2], Kanji Nagai[2], and Atsushi Ochiai[1]

[1]Pathology Division, Research Center for Innovative Oncology, National Cancer Center Hospital East, Kashiwa, Chiba, Japan; [2]Division of Thoracic Oncology, National Cancer Center Hospital East, Kashiwa, Chiba, Japan

ABSTRACT

Background. Cancer-associated fibroblasts (CAFs) directly communicate with cancer cells and play important roles in cancer progression. Recent studies have reported that primary cancer tissue with podoplanin-expressing CAFs predicted a poorer outcome among stage I lung adenocarcinoma patients. However, whether podoplanin(+)-CAFs also can be recruited into metastatic lymph nodes and influence the prognosis remains unclear.

Methods. We selected 112 patients with pathological N2 stage III lung adenocarcinoma and examined the podoplanin expression of CAFs and their prognostic impact in primary and metastatic N2 lesions.

Results. Podoplanin(+)-CAFs were observed in 61 (54.5 %) primary sites and 44 (39.3 %) metastatic lymph nodes. Podoplanin(+)-CAFs were found at metastatic lymph nodes in 33 (54.1 %) primary podoplanin-positive and 11 (21.6 %) primary podoplanin-negative sites. These findings suggest a significant positive correlation in podoplanin expression in CAFs between pairs of primary and metastatic lesions ($P < 0.001$). The difference in the overall survival of patients with podoplanin-positive/negative CAFs in their primary lesion was not correlated ($P = 0.927$). In contrast, patients with podoplanin(+)-CAFs in metastatic lymph nodes had a shorter overall survival than those without podoplanin(+)-CAFs ($P = 0.003$). In multivariate analyses, podoplanin(+)-CAFs in metastatic lymph nodes were a significantly independent risk factor for a poor outcome ($P = 0.007$).

Conclusions. Our study indicated that podoplanin(+)-CAFs in metastatic lymph nodes was a significant prognostic factor for overall survival among pathological N2 stage III adenocarcinoma patients.

Cancer tissue is composed of not only cancer cells but also different kinds of stromal cells. The main constituents of stromal cell are inflammatory cells, including lymphocytes, granulocytes, and macrophages, the endothelial cells of blood and lymph vessels, pericytes, and fibroblasts. These components create and orchestrate a favorable microenvironment for cancer cells and influence the survival of cancer cells in many types of cancer, such as breast cancer, pancreatic cancer, and lung cancer.[1–8] Fibroblasts, which acquire a specific biological phenotype via interaction with cancer cells, are known as cancer-associated fibroblasts (CAFs). The impact of certain types of CAFs on the biological behavior of cancer cells has been supported by extensive clinical evidence and the use of experimental mouse models.[9–15]

Human podoplanin is a 38 kDa type-1 transmembrane glycoprotein consisting of 162 amino acids, 9 of which

This work was supported by the Grant-in-Aid for Cancer Research (19-10) from the Ministry of Health, Labor, and Welfare Programs; the Foundation for the Promotion of Cancer Research, 3rd-Term Comprehensive 10-Year Strategy for Cancer Control; Program for Promotion of Fundamental Studies in Health Sciences of the National Institute of Biomedical Innovation.

Electronic supplementary material The online version of this article (doi:10.1245/s10434-012-2421-4) contains supplementary material, which is available to authorized users.

First Received: 3 September 2011;
Published Online: 6 June 2012

G. Ishii
e-mail: gishii@east.ncc.go.jp

A. Ochiai
e-mail: aochiai@east.ncc.go.jp

form the intracellular domain. The extracellular domain is highly *O*-glycosylated, with sialic acid, α-2, 3 linked to galactose, forming the main part of the protein's carbohydrate moieties.[16] We have reported previously that increased podoplanin expression in CAFs is correlated with a poor outcome among stage I lung adenocarcinoma patients.[17] Furthermore, in vitro and in vivo studies have revealed that these CAFs promote lung adenocarcinoma progression mediated by the podoplanin molecule.[18] These studies suggested that podoplanin-positive CAFs create a supportive microenvironment, enhancing tumor progression within the primary site. Another recent study has reported that a higher level of podoplanin expression in CAFs is correlated with a poor outcome in intrahepatic cholangiocarcinoma.[19]

Understanding the mechanism of tumor metastasis is essential not only for cancer biology but also for cancer treatment.[20] To gain insight into progression mechanism involving microenvironment at metastatic sites, in addition to primary sites, also is important. Practically, the sclerosis of metastatic lymph nodes often is observed among surgically resected samples, with the infiltration of numerous fibroblasts observed histologically. Furthermore, a recent study demonstrated that metastatic tumors may exert a paracrine effect on the recruitment of CAFs.[21] This possibility suggests that specific subtypes of CAFs may be recruited into metastatic lymph nodes. However, whether CAFs with the same phenotype as the primary sites are recruited into metastatic sites remains unclear.

In this study, we selected pathological N2 stage III lung adenocarcinoma patients and investigated whether a special subtype of CAFs at the primary sites was recruited into pair-matched metastatic sites in lymph nodes, focusing on podoplanin expression. Moreover, prognostic factors in pN2 stage III lung carcinoma remain unclear and controversial. We also examined the prognostic significance of the CAFs expressing podoplanin in the primary and metastatic sites.

MATERIALS AND METHODS

Patients

During the period from January 2001 to December 2007, a total of 1,925 consecutive patients with primary lung carcinoma underwent surgical resection at the National Cancer Center Hospital East, Chiba, Japan, and 1,628 patients received a complete resection (1,128 adenocarcinomas, 357 squamous cell carcinomas, 49 large cell carcinomas, 38 large cell neuroendocrine carcinomas, 28 adenosquamous carcinomas, and 28 others). We focused the adenocarcinoma patients to inspect the prognosis and selected the cases of 120 adenocarcinoma patients with pathological N2 stage III as potential candidates for inclusion in this study. The tumors were staged according to the International Union against Cancer's tumor-node-metastasis (TNM) classification 7th edition and were histologically subtyped and graded according to the World Health Organization (WHO) guidelines.[22,23] After excluding eight patients because they had received preoperative chemotherapy ($n = 1$) or because of the poor quality of the specimens that were obtained ($n = 7$), 112 patients were ultimately included in this study. The median follow-up period for these patients was 7.0 years. Survival time was measured from the date of surgery. All the patients signed an Institutional Review Board-approved informed consent form.

Pathological Studies

All the surgical specimens were fixed with 10 % formalin or 100 % methanol and embedded in paraffin. Serial 4-μm sections were stained with hematoxylin and eosin. Two observers (S.N. and G.I.) who were unaware of the clinical data independently reviewed all the pathological slides. The block containing the most extensive tumor component was selected from each primary tumor and metastatic N2 lymph nodes.

Evaluation of Clinicopathological Factors

Clinical characteristics were retrieved from the clinical records available. The following clinicopathological factors were investigated retrospectively to assess their correlation with podoplanin expression in the CAFs in primary and metastatic N2 lesions: sex, age, smoking history, preoperative serum carcinoembryonic antigen level, tumor differentiation, vascular invasion, lymphatic permeation, and pleural invasion.

Antibodies and Immunohistochemistry

Immunohistochemical staining was performed according to the procedure described in our previous report.[17] After antigen retrieval, individual slides were then incubated overnight at 4 °C using mouse anti-podoplanin antibody (D2-40; Convance, Emeryville, CA, USA) at a final dilution of 1:50, rabbit polyclonal anti-α-SMA (Actin, Smooth Muscle, Lab Vision, Fremont, CA, USA) at a final dilution of 1:100, and rabbit polyclonal anti-ZEB1 antibody (Anti-ZEB1, Sigma-Aldrich, St. Louis, MO, USA) at a final dilution of 1:250. The slides were washed three times with PBS and then incubated with EnVision™ (Dako, Denmark) for 1 h at room temperature. After washing with PBS, the color reaction was developed for 3 min in 2 % 3,3′-diaminobenzidine in 50 mM Tris-buffer

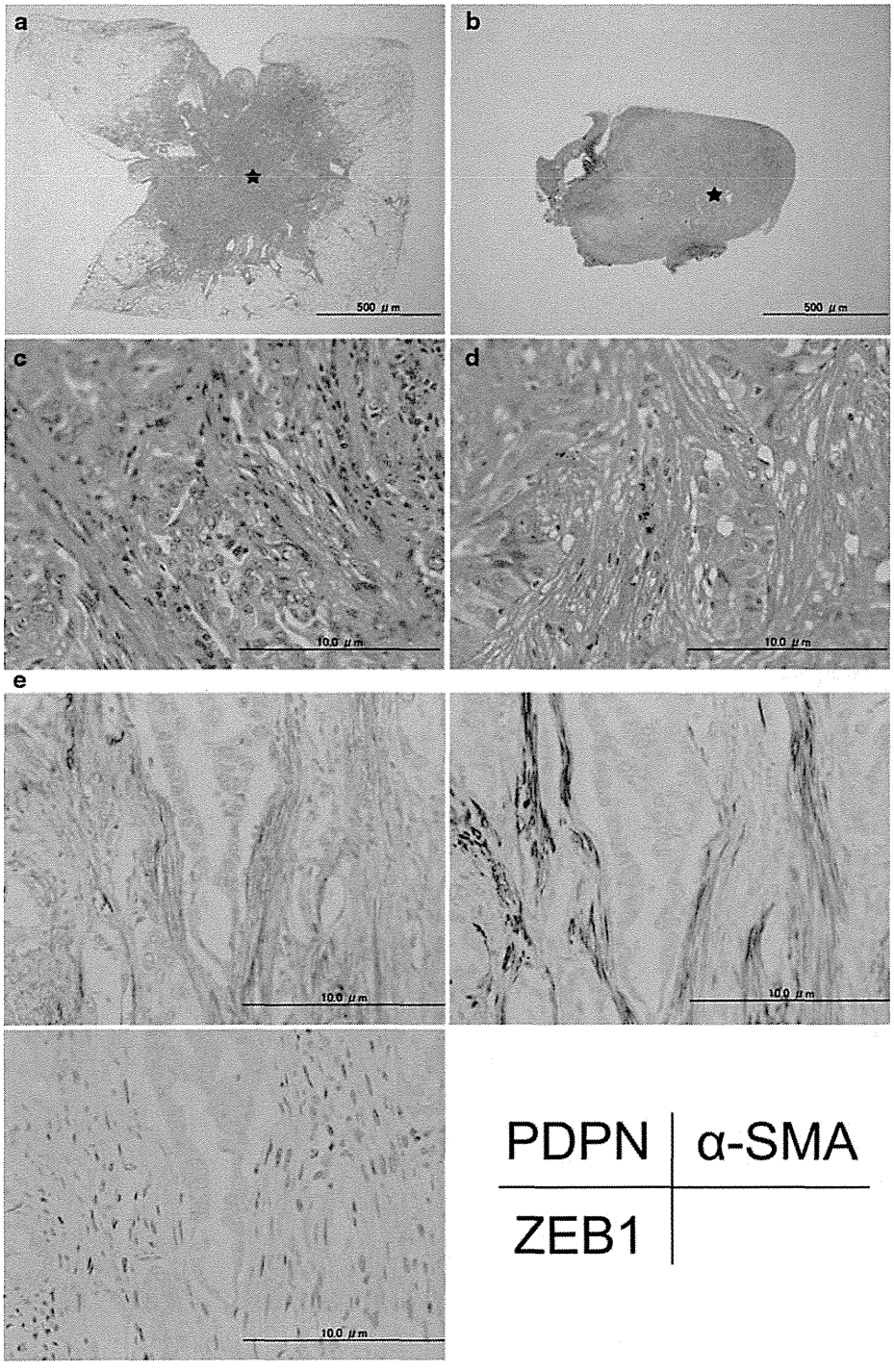

FIG. 1 Histological and immunohistological features of CAFs, and immunofluorescence analysis of podoplanin expression in CAFs, in primary lesions (**a, c, e, g**) and metastatic lesions (**b, d, f, h**). **a, b** Low-power field. Hematoxylin and eosin (HE) staining in primary and metastatic lesions. **c, d** High-power field. HE staining at the same sites of the stars in **a** and **b**, respectively. **e, f** Podoplanin, α-SMA and ZEB-1 expression in CAFs at the same primary and the same metastatic sites. **g, h** Results of double immunofluorescence staining at a primary site and a metastatic site. The *upper left* shows cells immunostained with anti-podoplanin antibody (D2-40). The *upper right* shows cells immunostained with α-SMA antibody. The *lower left* shows cells stained with DRAQ5^{TM} to identify nucleated cells. The *lower right* shows a composite of *images* obtained with both fluorophores

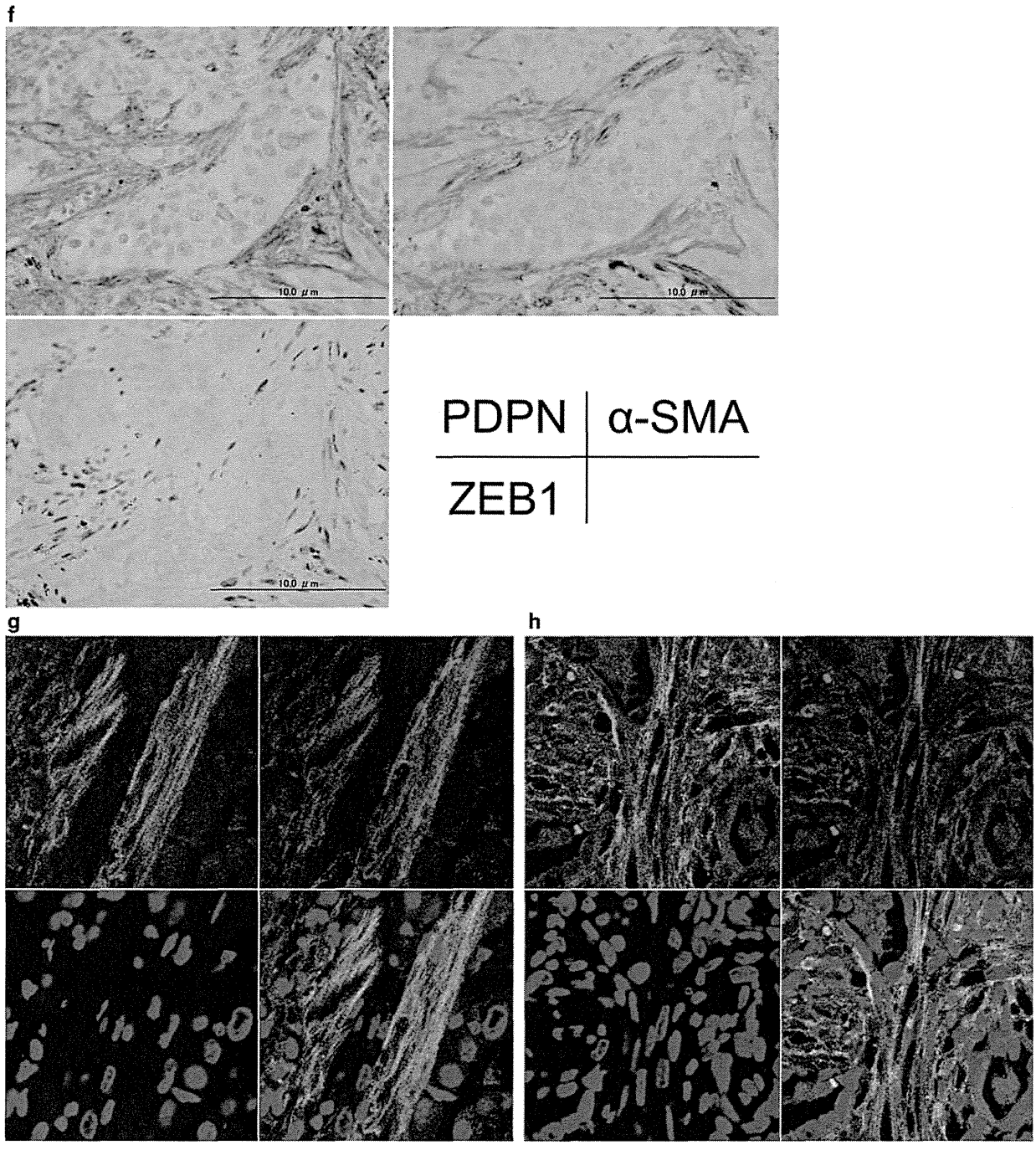

FIG. 1 continued

(pH 7.6) containing 0.3 % hydrogen peroxidase. Finally, the sections were counterstained with Meyer's hematoxylin, dehydrated, and mounted. The internal positive controls for podoplanin, α-SMA, and ZEB1 staining were lymphatic endothelial cells, vascular smooth muscle tissue, and fibroblast nuclei, respectively. We also performed negative control studies that were made without primary antigen in all antibodies. When at least 10 % of the stromal fibroblasts showed an unequivocally strong reaction that was the same as the strength of the reaction in lymphatic endothelial cells, the case was classified as podoplanin positive.[17]

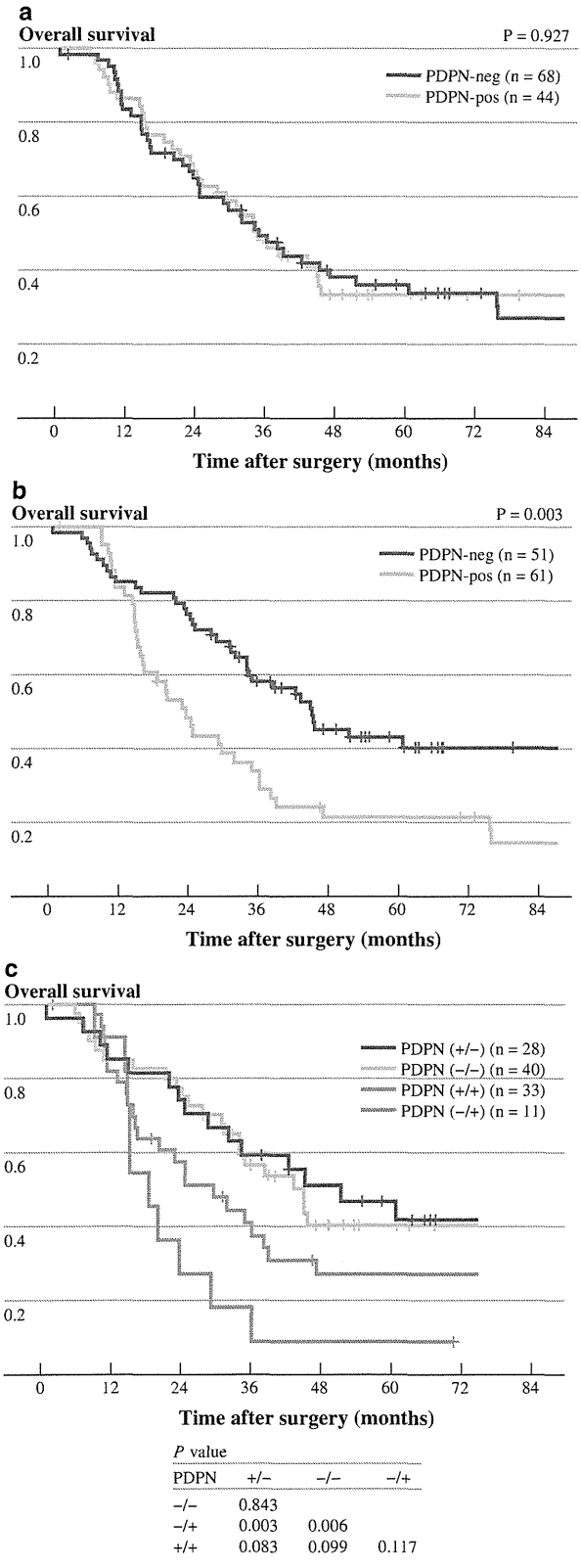

◀ **FIG. 2** Overall survival curves of podoplanin expression in CAFs in primary and metastatic lesions. **a** Overall survival curves of podoplanin expression in CAFs in primary lesions. **b** Overall survival curves of podoplanin expression in CAFs in metastatic lesions. **c** Overall survival curves of 4 groups according to the status of podoplanin expression in CAFs in primary/metastatic lesions (–/–, +/–, –/+ and +/+)

TABLE 1 Immunostaining results of CAFs for the anti-podoplanin antibody

Expression in metastatic lesions	*n*	PDPN expression in primary lesions		*P* value[a]
		Negative (%)	Positive (%)	
PDPN expression				
Negative	68	40 (78.4)	28 (45.9)	
Positive	44	11 (21.6)	33 (54.1)	<0.001

CAFs cancer-associated fibroblasts, *PDPN* podoplanin

[a] χ^2 test

Immunofluorescence and Confocal Microscopy

After incubating the sections with mouse anti-podoplanin antibody and rabbit polyclonal anti-α-SMA antibody, the sections were washed and either Alexa Fluor 488 goat anti-mouse IgG or Alexa Fluor 546 goat anti-rabbit IgG (Invitrogen, Carlsbad, CA, USA) was used as the secondary antibody. Before mounting, all the sections were stained with DRAQ5™ (Alexis Biochemical, Lausen, Switzerland) to identify nucleated cells. After mounting, the sections were examined by using an LSM5 Pascal confocal imaging system (Carl Zeiss, Jena, Germany), and then with an inverted microscope at an excitation wavelength of 488 nm for Alexa Fluor 488, 568 nm for Alexa Fluor 546, and 633 nm for DRAQ5™. Confocal images were stored as digital files and viewed using Photoshop software (Adobe, Mountain View, CA, USA).

Statistical Analysis

The correlations between podoplanin expression in the CAFs and the clinicopathological factors were evaluated using the χ^2 test. The primary and metastatic tumor sizes were assessed by using a Mann–Whitney *U* test. Survival time was measured from the date of surgery to the date of death or the date the patient was last known to be alive. The survival rates were estimated by using the Kaplan–Meier method, and the differences in survival curves were compared by log-rank test. The Cox proportional hazard model

TABLE 2 Relationship between podoplanin expression of CAFs in primary/metastatic lesions and clinicopathological factors

Variable	PDPN expression of CAFs					
	Primary lesions		*P* value[a]	Metastatic lesions		*P* value[a]
	Positive (%)	Negative (%)		Positive (%)	Negative (%)	
Age (yr)			0.85			0.699
≤65	25 (49)	31 (50.8)		21 (47.7)	35 (51.5)	
>65	26 (51)	30 (49.2)		23 (52.3)	33 (48.5)	
Gender			0.476			0.738
Male	31 (60.8)	33 (54.1)		26 (59.1)	38 (55.9)	
Female	20 (39.2)	28 (45.9)		18 (40.9)	30 (44.1)	
Smoking history			0.564			0.508
Never-smokers	19 (37.3)	26 (42.6)		16 (36.4)	29 (42.6)	
Smokers	32 (62.7)	35 (57.4)		28 (63.6)	39 (57.4)	
CEA (ng/ml)			0.850			0.053
≤5.0	26 (51)	30 (49.2)		17 (38.6)	39 (57.4)	
>5.0	25 (49)	31 (50.8)		27 (61.4)	29 (42.6)	
Differentiation			0.81			0.142
Well or moderately	37 (72.5)	43 (70.5)		28 (63.6)	52 (76.5)	
Poorly	14 (27.5)	18 (29.5)		16 (36.4)	16 (23.5)	
Vascular invasion			0.011			0.103
Absent	18 (35.3)	9 (14.8)		7 (15.9)	20 (29.4)	
Present	33 (64.7)	52 (85.2)		37 (84.1)	48 (70.6)	
Lymphatic permeation			0.182			0.122
Absent	23 (45.1)	20 (32.8)		13 (29.5)	30 (44.1)	
Present	28 (54.9)	41 (67.2)		31 (70.5)	38 (55.9)	
Pleural invasion			0.821			0.122
Absent	19 (37.3)	24 (39.3)		13 (29.5)	30 (44.1)	
Present	32 (62.7)	37 (60.7)		31 (70.5)	38 (55.9)	

CAFs cancer-associated fibroblasts, *CEA* preoperative serum carcinoembryonic antigen level, *PDPN* podoplanin

[a] χ^2 test

was used in univariate and multivariate analyses for overall survival. Before performing multivariate analyses, we assessed the multicollinearity of clinicopathological factors with reference to the *P* value of χ^2 test. If $P < 0.025$, we concluded that multicollinearity existed. When a statistically significant multicollinearity was found, the more important variable was retained for the multivariate analyses from clinical point of view. The multivariate analyses were performed as follows: first, Cox proportional hazard model regression, including aforementioned covariates, was performed focusing on podoplanin-expressing CAFs in primary lesions. Second, we conducted the same analysis focusing on those in metastatic lesions. Finally, Cox regression model, including interaction terms, was performed focusing on podoplanin expression of CAFs in both primary and metastatic lesions. Prognostic factors were identified using the criterion that $P < 0.05$, calculated from Cox proportional hazard model. All statistical analyses were performed using statistical software SPSS 11.0 (SPSS Inc., Chicago, IL, USA) and JMP 9 (SAS Institute, Cary, NC, USA).

RESULTS

Clinical Data

The median age of 112 patients was 65.5 (range, 41–83) years. Sixty-four patients (57.1 %) were male, and 48 (42.9 %) were female; 102 patients (91.1 %) underwent a lobectomy, and 10 (8.9 %) underwent a pneumonectomy. The number of patients with pathological stage IIIA and IIIB were 109 (97.3 %) and 3 (2.7 %). All three patients with pathological stage IIIB were T4 (pulmonary metastasis in another ipsilateral lobe).

Podoplanin Expression in CAFs in Primary and Metastatic N2 Lesions

The typical appearances of CAFs recruited into the primary (Fig. 1a, c) and the metastatic N2 (Fig. 1b, d) lesions are shown. Figure 1e showed the results of podoplanin, α-SMA (activated fibroblast marker), and ZEB1 (mesenchymal cell marker) expression on infiltrating

TABLE 3 Prognostic significance for overall survival (univariate Cox regression analysis)

Variable	*n*	Hazard ratio	95 % CI	*P* value
Age (yr)				
≤65	56	1		
>65	56	1.333	0.8426–2.1135	0.218
Gender				
Male	64	1		
Female	48	0.844	0.523–1.341	0.476
Smoking history				
Never-smokers	45	1		
Smokers	67	1.0655	0.671–1.718	0.79
CEA (ng/ml)				
≤5.0	56	1		
>5.0	56	1.309	0.828–2.073	0.248
Differentiation				
Well or moderately	80	1		
Poorly	32	1.207	0.504–1.418	0.48
Vascular invasion				
Absent	27	1		
Present	85	0.879	0.529–1.525	0.635
Lymphatic permeation				
Absent	43	1		
Present	69	1.576	0.979–2.611	0.062
Pleural invasion				
Absent	43	1		
Present	69	1.550	0.968–2.537	0.068
PDPN in primary lesions				
Negative	51	1		
Positive	61	1.022	0.644–1.636	0.927
PDPN in metastatic lesions				
Negative	68	1		
Positive	44	1.977	1.244–3.136	0.004

CEA preoperative serum carcinoembryonic antigen level, *CI* confidence interval, *PDPN* podoplanin

spindle cells within cancer stroma. The spindle cells were positive for these three markers, which indicated podoplanin-expressing CAFs. Figure 1f showed the staining of the pair-matched metastatic N2 lesion, which also indicated podoplanin expression by CAFs. Figure 1g and h showed the results of double immunofluorescence staining in the primary and metastatic lesions. The infiltrating spindle cells were positive for both podoplanin and α-SMA. Therefore, these spindle cells in the primary and metastatic tumors were morphologically and phenotypically identified as podoplanin-expressing CAFs.

Podoplanin-expressing CAFs were observed in 61 (54.5 %) primary lesions and 44 (39.3 %) metastatic lesions (Table 1). Thirty-three (54.1 %) of the 61 primary sites with podoplanin-expressing CAFs exhibited podoplanin expression in the CAFs at metastatic sites, and 11 (21.6 %) of the 51 primary sites without podoplanin-expressing CAFs had podoplanin expression in the CAFs at metastatic sites. The χ^2 test for podoplanin expression demonstrated a statistically positive correlation ($P < 0.001$) for the pairs of primary and metastatic lesions. The median primary tumor size was 3.2 (range, 1.3–8.0) cm in podoplanin expressing CAF-negative lesions and 3.2 (range, 1.0–7.8) cm in podoplanin expressing CAF-positive lesions. The sizes of the primary tumors in the podoplanin positive and negative lesions were not statistically different (Mann–Whitney test, $P = 0.939$). The median metastatic N2 tumor size was 6.0 (range, 1.0–25.0) mm in podoplanin expressing CAF-negative lesions and 9.0 (range, 1.5–23.0) mm in podoplanin expressing CAF-positive lesions. The sizes of the metastatic tumors in the podoplanin-positive and -negative lesions were not statistically different (Mann–Whitney test, $P = 0.094$).

Podoplanin Expression in CAFs in Metastatic Lesions was Significantly Correlated with a Shorter Survival Time in pN2 Lung Adenocarcinoma Cases

The relationship between podoplanin expression in CAFs in primary and metastatic N2 lesions and clinicopathological factors are shown in Table 2. Statistical association between podoplanin expression in the primary lesions and vascular invasion was verified (χ^2 test, $P = 0.011$).

Univariate analyses were performed according to the Cox proportional hazard model to determine the prognostic value of podoplanin expression in CAFs in primary and metastatic lesions (Table 3). Podoplanin expression in CAFs in metastatic lesions was statistically correlated with a shorter survival time ($P = 0.004$), whereas podoplanin expression in CAFs in primary lesions was not correlated with a shorter survival time ($P = 0.927$).

As a result of avoiding multicollinearity, vascular invasion and gender were excluded from multivariate analyses, because statistically strong correlations were identified between vascular invasion and pleural invasion, and podoplanin expression in CAFs in primary lesions (χ^2 test, $P = 0.013$, 0.011, respectively), and between gender and smoking history (χ^2 test, $P < 0.001$). The multivariate Cox regression analysis focusing on podoplanin expression in primary lesions showed that podoplanin-expressing CAFs in primary sites was not associated with shorter overall survival ($P = 0.913$, hazard ratio (HR) 1.027, 95 % confidence interval (CI) 0.638–1.666; Supp. Table 1a). On the contrary, the multivariate Cox regression analysis focusing on podoplanin expression in metastatic sites

TABLE 4 Prognostic significance for overall survival (multivariate Cox regression analysis of podoplanin-expressing CAFs in primary and metastatic lesions)

Variable	*n*	Hazard ratio	95 % CI	*P* value
Age (yr)				
≤65	56	1		
>65	56	1.491	0.919–2.426	0.103
Smoking history				
Never-smokers	45	1		
Smokers	67	1.141	0.704–1.879	0.601
CEA (ng/ml)				
≤5.0	56	1		
>5.0	56	1.184	0.733–1.914	0.48
Differentiation				
Well or moderately	80	1		
Poorly	32	1.12	0.643–1.878	0.672
Lymphatic permeation				
Absent	43	1		
Present	69	1.372	0.827–2.334	0.227
Pleural invasion				
Absent	43	1		
Present	69	1.283	0.765–2.189	0.309
PDPN in primary lesions				
Negative	51	1		
Positive	61	0.77	0.465–1.292	0.309
PDPN in metastatic lesions				
Negative	68	1		
Positive	44	2.058	1.218–3.437	0.007
PDPN in primary lesions * PDPN in metastatic lesions interaction				0.399

CEA preoperative serum carcinoembryonic antigen level, *CI* confidence interval, *PDPN* podoplanin

showed that podoplanin-expressing CAFs in metastatic lesions was associated with shorter overall survival ($P = 0.017$, HR 1.8, 95 % CI 1.112–2.908; Supp. Table 1b). Podoplanin-expressing CAFs in metastatic sites was correlated with poorer overall survival in the multivariate analysis, including podoplanin expression in both primary and metastatic lesions ($P = 0.007$, HR 2.061, 95 % CI 1.221–3.44; Table 4). The interaction terms of podoplanin expression in CAFs in primary and metastatic lesions showed no clear association on overall survival (interaction $P = 0.399$). Only podoplanin expression in CAFs in metastatic lesions was a significantly independent prognostic factor for overall survival.

The overall survival curves obtained using the Kaplan–Meier method, with statistical significance assessed by using the log-rank test, are shown in Fig. 2. The difference in the overall survival time of the patients whose CAFs in the primary lesions were podoplanin-positive or -negative was not significant ($P = 0.927$; Fig. 2a). The estimated 5-year survival rates were 36.1 and 33.4 %, respectively. The overall survival time of the patients whose CAFs in the metastatic lesions were positive were significantly shorter than those of the patients whose CAFs were negative ($P = 0.003$; Fig. 2b). The estimated 5-year survival rates were 21.5 and 43.1 %, respectively. We divided the cases into four groups according to the status of podoplanin expression in CAFs. In the four groups without/with podoplanin-expressing CAFs in primary/metastatic lesions (−/−, +/−, −/+ and +/+), the estimated 5-year survival rates were 40.2 % ($n = 40$), 46.8 % ($n = 28$), 9.1 % ($n = 11$), and 26.9 % ($n = 33$), respectively (Fig. 2c). Sixty-one cases (82.4 %; 61/74) died of lung cancer.

DISCUSSION

This is the first report to describe the specific relationship between primary and metastatic microenvironments with reference to the existence of podoplanin-positive CAFs. In this study, we found that cancer cells can recruit a special subtype of CAFs, podoplanin expressing CAFs, into metastatic lymph nodes. CAFs expressing podoplanin demonstrated a significant, positive correlation for pairs of primary and metastatic sites. Moreover, cases with the presence of podoplanin expressing CAFs not at the primary

sites but at the metastatic sites had a significantly poorer outcome according to univariate and multivariate analyses in pN2 stage III.

The biological function of podoplanin expression in CAFs has not yet been fully investigated. We recently demonstrated that podoplanin-positive fibroblasts displayed enhanced tumor formation, lymph node metastasis, and lung metastasis in a human lung adenocarcinoma cell line, A549, compared with podoplanin-negative fibroblasts in animal models.[18] Furthermore, the knockdown of podoplanin in fibroblasts decreased the augmenting effect of tumor formation in mice and in vitro colony formation.[18] The in vitro colony assay also suggested that podoplanin on fibroblasts promoted an environment conductive to cancer cell anchorage independence, regardless of angiogenesis or inflammation.[18] These results indicated that podoplanin on fibroblasts was a functional protein in tumor formation enhancement.[18] Taken together, these results suggest that a metastatic microenvironment created by both podoplanin expressing CAFs and cancer cells may confer the additional malignant potential of metastasized cancer cells, such as the migration, proliferation, survival, and resistance of chemotherapy treatment.

Normal lymph nodes consist of lymphatic tissues enclosed by a fibrous capsule and do not originally contain fibroblasts.[24] In this study as well, we could not find any fibroblasts within normal lymph nodes. The origins of recruited CAFs in metastatic lymph nodes are controversial. Ishii et al. reported that circulating fibroblast progenitor cells derived from bone marrow can be recruited into cancer tissue implanted in the skin of severe combined immunodeficient mice.[25] On the other hand, Duda et al. recently demonstrated that metastatic CAFs can be derived from primary CAFs accompanied by primary cancer cells.[26] These results indicated that CAFs in metastatic lymph nodes may be released from external tissue, such as primary lesions, and anchored there. Moreover, podoplanin is expressed in the follicular dendritic cells of lymph nodes.[27] Dendritic cells also may transdifferentiate into CAFs and retain podoplanin expression. A further challenge is to clarify the origins of CAFs using experimental models.

Some studies have reported that skip N2 metastasis and the highest level of metastasis to the mediastinal lymph nodes were identified as significant prognostic factors.[28,29] In this study, skip N2 or single station metastasis were not correlated with the outcome (data not shown). Our study demonstrated that podoplanin-expressing CAFs recruited into metastatic sites may be a markedly significant risk factor for a poor outcome, although the tumor size of metastatic lymph nodes was not related to podoplanin expression in the CAFs. Therefore, examining podoplanin expression in CAFs at metastatic sites may be of clinical importance for determining the management or prognosis of pN2 stage III adenocarcinoma patients.

In our previous study, we found that an increase in podoplanin expression in CAFs at primary sites was correlated with a poor outcome for all stages, especially stage I.[17] The cases used in the present study were all pN2 stage III cases, and this study showed that podoplanin expression in CAFs in primary lesions was not significantly correlated with outcome. Because the prognosis of advanced lung adenocarcinoma is basically very poor, a microenvironment could be an independent prognostic risk factor not at the primary sites but at the metastatic sites. Podoplanin expression by CAFs in metastatic lesions might enhance the colonization of cancer cells, develop tumor progression, and influence the prognosis.

In conclusion, the current study suggested the possible involvement of the same tumor soil (recruitment of podoplanin-expressing CAFs) in both primary and metastatic N2 lesions and the importance of a special microenvironment in metastatic lymph nodes for the prognosis. Our current results imply that strategies that are directed to block the recruitment and tumor-associated functions of podoplanin-expressing CAFs may be an effective treatment. Further molecular studies on the role of these "educated fibroblasts" should provide novel insights into the pathogenesis of the unique microenvironment for cancers at both primary and metastatic sites.

ACKNOWLEDGMENT The authors thank Mr. Shogo Nomura for statistical advice and Mr. Shinya Yanagi for technical support. This work was supported by the Grant-in-Aid for Cancer Research (19-10) from the Ministry of Health, Labor, and Welfare Programs; the Foundation for the Promotion of Cancer Research, 3rd-Term Comprehensive 10-Year Strategy for Cancer Control; Program for Promotion of Fundamental Studies in Health Sciences of the National Institute of Biomedical Innovation.

REFERENCES

1. Baglole CJ, Ray DM, Bernstein SH, et al. More than structural cells, fibroblasts create and orchestrate the tumor microenvironment. *Immunol Invest.* 2006;35:297–325.
2. Bissell MJ, Radisky D. Putting tumours in context. *Nat Rev Cancer.* 2001;1:46–54.
3. Hanahan D, Weinberg RA. The hallmarks of cancer. *Cell.* 2000;100:57–70.
4. Kalluri R, Zeisberg M. Fibroblasts in cancer. *Nat Rev Cancer* 2006;6:392–401.
5. Mantovani A, Allavena P, Sica A, et al. Cancer-related inflammation. *Nature.* 2008;454:436–44.
6. Morrissey C, Vessella RL. The role of tumor microenvironment in prostate cancer bone metastasis. *J Cell Biochem.* 2007;101: 873–86.
7. Patocs A, Zhang L, Xu Y, et al. Breast-cancer stromal cells with TP53 mutations and nodal metastases. *N Engl J Med.* 2007;357: 2543–51.
8. Tlsty TD, Coussens LM. Tumor stroma and regulation of cancer development. *Annu Rev Pathol.* 2006;1:119–50.

9. Desmouliere A, Guyot C, Gabbiani G. The stroma reaction myofibroblast: a key player in the control of tumor cell behavior. *Int J Dev Biol.* 2004;48:509–17.
10. Orimo A, Gupta PB, Sgroi DC, et al. Stromal fibroblasts present in invasive human breast carcinomas promote tumor growth and angiogenesis through elevated SDF-1/CXCL12 secretion. *Cell.* 2005;121:335–48.
11. Pietras K, Pahler J, Bergers G, et al. Functions of paracrine PDGF signaling in the proangiogenic tumor stroma revealed by pharmacological targeting. *PLoS Med.* 2008;5:e19.
12. Allinen M, Beroukhim R, Cai L, et al. Molecular characterization of the tumor microenvironment in breast cancer. *Cancer Cell.* 2004;6:17–32.
13. Cui L, Ohuchida K, Mizumoto K, et al. Prospectively isolated cancer-associated CD10(+) fibroblasts have stronger interactions with CD133(+) colon cancer cells than with CD133(−) cancer cells. *PLoS One.* 2010;5:e12121.
14. Nakao M, Ishii G, Nagai K, et al. Prognostic significance of carbonic anhydrase IX expression by cancer-associated fibroblasts in lung adenocarcinoma. *Cancer.* 2009;115:2732–43.
15. Bremnes RM, Donnem T, Al-Saad S, et al. The role of tumor stroma in cancer progression and prognosis: emphasis on carcinoma-associated fibroblasts and non-small cell lung cancer. *J Thorac Oncol.* 2011;6:209–17.
16. Wicki A, Christofori G. The potential role of podoplanin in tumour invasion. *Br J Cancer.* 2007;96:1–5.
17. Kawase A, Ishii G, Nagai K, et al. Podoplanin expression by cancer associated fibroblasts predicts poor prognosis of lung adenocarcinoma. *Int J Cancer.* 2008;123:1053–9.
18. Hoshino A, Ishii G, Ito T, et al. Podoplanin-positive fibroblasts enhance lung adenocarcinoma tumor formation. *Cancer Res.* 2011;71:4769–79.
19. Aishima S, Nishihara Y, Iguchi T, et al. Lymphatic spread is related to VEGF-C expression and D2-40-positive myofibroblasts in intrahepatic cholangiocarcinoma. *Mod Pathol.* 2008;21:256–64.
20. Coghlin C, Murray GI. Current and emerging concepts in tumour metastasis. *J Pathol.* 2010;222:1–15.
21. Vered M, Dayan D, Yahalom R, et al. Cancer-associated fibroblasts and epithelial-mesenchymal transition in metastatic oral tongue squamous cell carcinoma. *Int J Cancer.* 2010;127:1356–62.
22. Goldstraw P, Crowley J, Chansky K, et al. The IASLC Lung Cancer Staging Project: proposals for the revision of the TNM stage groupings in the forthcoming (seventh) edition of the TNM Classification of malignant tumours. *J Thorac Oncol.* 2007;2:706–14.
23. Travis WD, Brambilla E, Müller-Hermelink HK, et al., editors. Tumours of the lung, pleura, thymus and heart. Lyon: IARC Press; 2004.
24. Kumar V, Abbas AK, Fausto N. Robbins and Cotran pathologic basis of disease. 7th ed. Philadelphia: W.B. Saunders; 2004.
25. Ishii G, Sangai T, Sugiyama K, et al. In vivo characterization of bone marrow-derived fibroblasts recruited into fibrotic lesions. *Stem Cells.* 2005;23:699–706.
26. Duda DG, Duyverman AM, Kohno M, et al. Malignant cells facilitate lung metastasis by bringing their own soil. *Proc Natl Acad Sci USA.* 2010;107:21677–82.
27. Xie Q, Chen L, Fu K, et al. Podoplanin (d2-40): a new immunohistochemical marker for reactive follicular dendritic cells and follicular dendritic cell sarcomas. *Int J Clin Exp Pathol.* 2008;1:276–84.
28. Ohta Y, Shimizu Y, Minato H, et al. Results of initial operations in non-small cell lung cancer patients with single-level N2 disease. *Ann Thorac Surg.* 2006;81:427–33.
29. Nakagiri T, Sawabata N, Funaki S, et al. Validation of pN2 subclassifications in patients with pathological stage IIIA N2 non-small cell lung cancer. *Interact Cardiovasc Thorac Surg.* 2011;12:733–8.

Cancer Science
The official journal of the Japanese Cancer Association JCA

Morphophenotypic characteristics of intralymphatic cancer and stromal cells susceptible to lymphogenic metastasis

Yuki Matsumura,[1,2] Genichiro Ishii,[1,3] Keiju Aokage,[1,2] Takeshi Kuwata,[1] Tomoyuki Hishida,[2] Junji Yoshida,[2] Mitsuyo Nishimura,[2] Kanji Nagai[2] and Atsushi Ochiai[1,3]

[1]Pathology Division, Research Center for Innovative Oncology, Chiba; [2]Division of Thoracic Surgery, National Cancer Center Hospital East, Chiba, Japan

(Received December 19, 2011/Revised March 2, 2012/Accepted March 12, 2012/Accepted manuscript online March 16, 2012/Article first published online April 23, 2012)

The intravessel microenvironment has significant effects on cancer metastasis. The aim of the present study was to determine how the morphologic and immunophenotypic features of cancer cells and infiltrating stromal cells within the permeated lymphatic vessels are associated with lymphogenic metastasis. A total of 137 primary lung adenocarcinoma patients with extratumoral lymphatic permeations were examined. Morphologically, the floating cancer nests within the permeated lymphatic vessels were divided into two types: Type A, consisting of a single large cancer nest; and Type B, consisting of multiple small cancer nests. We compared the clinicopathologic characteristics and the immunophenotypes of the cancer cells and infiltrating stromal cells between the Type A and Type B nests. Eleven of 54 Type A patients (20%) had intrapulmonary metastases, compared with 36 of 83 Type B patients (43%; $P = 0.006$). Immunohistochemically, Type B cancer cells expressed significantly higher levels of CD44 than Type A cancer cells (mean scoresAUTHOR: Scores - what is this score? Is it the number of cells expressing CD44 or the concentration of CD44 or some other type of scoring system? 43.0 *vs* 20.5, respectively) and E-cadherin (60.5 *vs* 31.5, respectively), but lower levels of Geminin (11.9% *vs* 20.3%, respectively) and cleaved caspase 3 (2.4% *vs* 7.8%AUTHOR: 11.9% vs 20.3%, respectively) and cleaved caspase 3 (2.4% vs 7.8%, – what do the percentages here refer to? The number of cells expressing geminin and caspase 3? The levels of these factors? Please clarify., respectively). Moreover, a significantly larger number of CD204-positive macrophages were present within the cancer-permeated lymphatic vessels in Type B patients than in Type A patients (mean number 9.5 *vs* 4.6, respectively). The present study reveals that intralymphatic cancer cell and stromal cell phenotypes are susceptible to lymphogenic metastasis, suggesting that lymphogenic metastasis may be affected by the intralymphatic microenvironment they create. (*Cancer Sci* 2012; 103: 1342–1347)

The cause of death in most cancer patients is the development of metastases from the primary tumor. The metastatic process includes various complex steps. The process starts with the separation of cancer cells from the primary lesion, followed by the permeation of these cells into vessels. In permeated vessels, the cancer cells survive apoptosis (a process known as anoikis), proliferate, and then transmigrate to the metastatic site. Thereafter, the tumor cells adhere to the endothelial cells and extravasate to the connective tissues surrounding the vessels. By interacting with the stromal cells present in that location, they finally invade the target organ parenchyma, followed by the development of metastatic lesions. We recently reported that, after extravasation from lymphatic vessels, cancer cells undergo a dynamic phenotypic change associated with the epithelial–mesenchymal transition (EMT) within the connective tissue of the vessel wall.[1] The cellular and molecular mechanisms involved in each process have been the topic of constant debate and have inspired extensive research.

One study focusing on the location of lymphatic permeation in resected non-small cell lung cancers found that extratumoral lymphatic permeation was an independent prognostic factor.[2] That study report implied that extratumoral lymphatic vessels are an important metastatic route. Sakuma *et al.*[3], using lung adenocarcinoma cell lines, reported that tumor cells floating in lymphatic vessels resist anoikis by expressing phosphorylated (p-) Src. Conversely, recent reports have revealed the presence of circulating stromal cells that associate with cancer cells and play a role in cancer cell survival, proliferation, and invasion. Ishii *et al.*[4] advocated that the blood in the vicinity of human lung cancers contains fibroblast progenitor cells that have the capacity to migrate into the cancer stroma and differentiate into stromal fibroblasts. Duda *et al.*[5] also revealed that tumor-associated stromal cells shed from the primary tumor together with accompanying cancer cells survive in the blood circulation, as well as at secondary sites, and proliferate within the metastatic nodules. Together, these results suggest that the metastatic process may be affected not only by the characteristics of floating cancer cells, but also by those of circulating stromal cells.

We hypothesized that the intralymphatic microenvironment created by tumor cells and stromal cells has a considerable influence on the metastatic process and that the phenotypes of the tumor cells and infiltrating stromal cells in extratumoral lymphatic vessels may be informative for research into the mechanism of cancer metastasis, including intrapulmonary metastasis. We noted the high prevalence of intrapulmonary metastasis among patients with extratumoral lymphatic permeation of lung adenocarcinoma. The aim of the present study was to determine how the morphologic and immunophenotypic features of tumor cells and infiltrating stromal cells within permeated lymphatic vessels are associated with intrapulmonary metastasis.

Materials and Methods

Patient selection. Between July 1992 and May 2010, 2016 patients with primary lung adenocarcinoma underwent surgical resection at the National Cancer Center Hospital East, Chiba, Japan. After reviewing the medical records, 137 patients with extratumoral lymphatic permeations were chosen for as subjects for the present study.

Histological studies. Surgical specimens were fixed in 10% formalin or 100% methyl alcohol. The specimens were sliced

[3]To whom correspondence should be addressed.
E-mail: gishii@east.ncc.go.jp; aochiai@east.ncc.go.jp

doi: 10.1111/j.1349-7006.2012.02275.x

through the largest diameter of the primary tumor and all sections were embedded in paraffin. We also identified all peripheral subsegmental bronchi and obtained sections containing subsegmental bronchi even in sections without the primary tumor. These sections were also embedded in paraffin. The median number of tissue blocks was 21 pieces for each case. All serial 4-μm sections were stained using H&E, the Alcian blue–periodic acid-Schiff (AB-PAS) method for the detection of cytoplasmic mucin production, or the Elastica van Gieson (EVG) or Victoria–blue van Gieson (VVG) methods for the detection of elastic fibers. All histological materials included in this series were reviewed by two pathologists (YM and GI) to ascertain the presence of extratumoral lymphatic permeation and intrapulmonary metastasis (PM), as well as to assess the histopathological features of both the primary and metastatic tumors. A PM was defined as an independent tumor having the same histopathological features, including the growth pattern, cell size, and nuclear atypia, as the primary tumor and was differentiated from synchronous multiple primary lung cancer.[6] Metastatic nodules that had apparently occurred as a result of aerogenous spreading were excluded from the present study. As a result, 47 of 137 patients were found to have PM. The pathological stage was determined based on the TNM classification of the International Union Against Cancer (renamed Union for International Cancer Control [UICC]).[7] Histological typing of the primary tumors was performed based on World Health Organization classification of cell types,[8] and the types were divided into five subtypes as follows: bronchioloalveolar carcinoma (BAC) (non-mucinous BAC or mucinous BAC), acinar, papillary, solid adenocarcinoma with mucin production, and mixed subtype.[8] Lymphatic permeation was confirmed in all 137 patients based on findings for both H&E- and D2-40-stained sections, with the latter used to evaluate lymphatic endothelial cells. Extratumoral lymphatic permeation was defined as tumor cells existing in the lymphatic vessels outside the primary tumors. Vascular invasion was considered to be present when tumor cells in the blood vessels were identified on EVG- or VVG-stained sections. Pleural invasion was also evaluated based on whether the tumor cells had invaded the visceral pleura of the lung on EVG- or VVG-stained sections.

Morphological assessment of tumor cell nests within lymphatics. Microscopic examinations revealed that tumor nests within extratumoral lymphatic vessels can be divided into two morphologic patterns based on the structure of the nest: (i) "Type A", defined as tumor cells in the permeated lymphatic vessels forming a single large mass without separation (Fig. 1a); and (ii) "Type B", defined as tumor cells in the permeated lymphatic vessels arranged in multiple small clusters (Fig. 1b). More concretely, we defined Type A as having one large cluster consisting of 20 or more combined cancer cells within permeated lymphatic vessels. Even if many cancer cells exist in the lymphatic vessels, small clusters of <20 cancer cells were classified as Type B. When both morphologic patterns were observed in the same section, we adopted the dominant one.

Antibodies and immunohistochemical staining. The markers of cell proliferation and anoikis resistance used in the present study were Gemini (clone EM6; Novocastra, Newcastle-upon-Tyne, UK), cleaved caspase 3 (polyclonal; Cell Signaling Technology, Danvers, MA, USA), and p-Src ($pTyr^{416}$, polyclonal; Calbiochem, Darmstadt, Germany). The markers of adhesion-related molecules were CD44 (clone DF1485; Novocastra), E-cadherin (clone 36; BD Biosciences, San Jose, CA, USA), and fibronectin (clone 568; Leica Microsystems, Newcastle, UK). To evaluate growth factors, we used epithelial growth factor receptor (EGFR; clone H11; Dako Cytomation, Glostrup, Denmark) and insulin-like growth factor receptor (IGFR; Chemicon, Temecula, CA, USA). To evaluate T lymphocytes, B lymphocytes, and activated macrophages, we used CD3 (Leica Microsystems), CD79a (Leica Microsystems), and CD204 (clone SRA-E5; Trans Genic, Hyogo, Japan), respectively. Podoplanin (clone D2-40; Signet, Princeton, NJ, USA) was used as a lymphatic endothelial marker and carbonic anhydrase IX (CA-IX, polyclonal; Novus Biologicals, Littleton, CO, USA) was used as a marker of hypoxia. Immunostaining was performed on 4-μm paraffin-embedded tissue sections. Slides were deparaffinized in xylene and dehydrated in a graded ethanol series, and endogenous peroxidase was blocked with 3% hydrogen peroxide in absolute methyl alcohol. After epitope retrieval, the slides were washed with PBS and incubated overnight with primary antibodies. The reaction products were stained with diaminobenzidine and counterstained with hematoxylin.

Immunohistochemical scoring. All stained tissue sections were scored semiquantitatively and evaluated independently under a

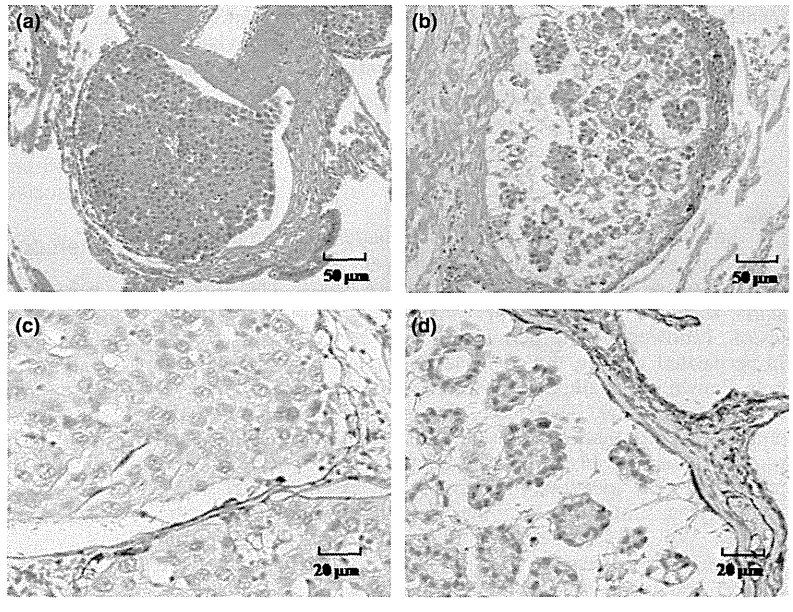

Fig. 1. Morphologic patterns of cancer cell nests within lymphatic vessels. (a,b) Hematoxylin–eosin staining of a "Type A" nest (a) and a "Type B" nest (b). In the Type A nest, tumor cells within the lymphatic vessels form a single large mass without separation, whereas in the Type B nest the tumor cells within the lymphatic vessels are arranged in multiple small clusters. (c,d) Staining using an anti-D2–40 antibody to evaluate Type A (c) and Type B (d) tumor cell nests within lymphatic vessels.

light microscope by two pathologists (YM and GI) who had no knowledge of the patients' clinicopathological data. The labeling scores for the tumor cells within extratumoral lymphatics were calculated by multiplying the percentage of positive tumor cells per each lesion (0–100%) by the staining intensity level (0 = negative; 1 = weak; 2 = strong). For Geminin and cleaved caspase 3, the number of positive tumor cells per 100 tumor cells was counted. For CD3, CD79a and CD 204, the number of positive infiltrating cells was counted under a microscopic at × 400 (area = 0.0625 mm^2). We confirmed that positive control tissues were stained by each antibody and we also performed negative control studies without the primary antigen for all antibodies. When the antibody evaluations differed, the observers discussed the results, re-examining the slides if necessary, until an agreement was reached.

Statistical analysis. The significance of differences between two groups was evaluated using the Mann–Whitney *U*-test or Fisher's exact test. All *P*-values reported are two sided, and the significance level was set at <0.05. Analyses were performed using Dr. SPSS II for Windows, standard version 11.0 (SPSS, Chicago, IL, USA).

Results

Clinicopathologic findings of patients with extratumoral lymphatic permeation. The clinicopathologic characteristics of 137 patients who had adenocarcinoma with extratumoral lymphatic permeation ($Ly^{ext}(+)$) and the other 1879 patients are given in Table 1. Men, ex or current smokers, patients with high serum carcinoembryonic antigen (CEA) levels, those with pathological T2–3, and pleural invasion were significantly more likely to be $Ly^{ext}(+)$. Furthermore, significantly more cases with lymph node metastasis (pN1–2) and PM were found among the $Ly^{ext}(+)$ patients.

Morphological patterns of tumor nests within extratumoral lymphatic vessels. The tumor nests within the lymphatic vessels were divided morphologically into two groups, Type A and Type B. Fifty-four patients were found to have "Type A" tumor nests (i.e. tumor cells formed a large solid nest within the permeated lymphatic vessels; Fig. 1a,c). Eighty-three patients were found to have "Type B" tumor nests (i.e. tumor cells were arranged in multiple small clusters within the permeated lymphatic vessels; Fig. 1b,d). When both morphologic patterns were observed in the same section, we adopted the dominant one. Figure S1, available as Supplementary Material to this paper, shows the distribution of cases with extratumoral lymphatic permeation according to the rate of Type A and Type B tumor nests. There were 36 patients with 100% Type A tumor nests, 25 with 100% Type B tumor nests, and 76 patients with mixed Type A and Type B tumor nests. Patients with 50% of both type (n = 7) were classified as having Type B tumor nests. Table 2 gives the clinicopathologic characteristics of patients with Type A and Type B tumor nests. In the group in which Type B tumor nests were dominant, significantly more patients had a papillary predominant pattern and PM, whereas fewer patients had a solid predominant pattern, compared with the Type A group.

Clinicopathologic factors related to PM. The clinicopathologic characteristics of cases with or without PM are summarized in Table 3. No significant differences in gender, age, smoking history, CEA, primary tumor size, pathological N status, or pleural invasion were observed between the two groups, but

Table 1. Clinicopathological characteristics of all patients

	$Ly^{ext}(+)$ (n = 137)	$Ly^{ext}(-)$ (n = 1879)	*P*-value
Gender			
Men (*n*)	92	961	<0.001
Women (*n*)	45	918	
Age range (years)	41–84	20–92	
Median age (years)	66	65	
Smoking habit			
Never smoked (*n*)	45	842	0.009
Ex or current smoker (*n*)	92	1018	
Carcinoembryonic antigen (ng/mL)			
≤5 (*n*)	71	1231	0.0017
>5 (*n*)	66	640	
Median tumor size (cm)	3.0	2.5	0.006
T status			
pT1 (*n*)	32	981	
pT2–4 (*n*)	105	898	<0.001
N status			
pN0 (*n*)	21	1382	<0.001
pN1–2 (*n*)	110	423	
Pleural invasion			
No (*n*)	53	1341	<0.001
Yes (*n*)	85	538	
Intrapulmonary metastasis			
No (*n*)	90	1763	<0.001
Yes (*n*)	47	116	

Ly^{ext}, extratumoral lymphatic permeation.

Table 2. Clinicopathological characteristics of Type A- and Type B-dominant patients

	Type A dominant (n = 54)	Type B dominant (n = 83)	*P*-value
Gender			
Men (*n*)	40	52	0.20
Women (*n*)	14	31	
Age range (years)	42–84	42–82	0.58
Median age (years)	65	64	
Smoking habit			
Never smoked (*n*)	14	31	0.20
Ex or current smoker (*n*)	40	52	
Carcinoembryonic antigen (ng/mL)			
≤5 (*n*)	30	41	0.49
>5 (*n*)	24	42	
Tumor size (cm)	1–16	1.2–12	0.29
Median size (cm)	3.2	2.8	
Predominant subtype			
Lepidic growth pattern (*n*)	2	3	0.65
Acinar (*n*)	12	17	0.48
Papillary (*n*)	9	48	<0.01
Micropapillary (*n*)	0	0	–
Solid (*n*)	31	15	<0.01
Pathological T status			
pT1 (*n*)	14	18	0.35
pT2 (*n*)	27	30	
pT3–4 (*n*)	13	35	
Pathological N status			
pN0 (*n*)	12	14	0.51
pN1–2 (*n*)	42	69	
Pleural invasion			
No (*n*)	20	33	0.86
Yes (*n*)	34	50	
Intrapulmonary metastasis			
No (*n*)	43	47	<0.01
Yes (*n*)	11	36	

Ly^{ext}, extratumoral lymphatic permeation.

doi: 10.1111/j.1349-7006.2012.02275.x

the group with PM contained significantly more cases with a Type B morphologic pattern than a Type A pattern. These results suggest that the morphologic characteristics of the tumor cell nests within the extratumoral lymphatics are closely related to PM.

Immunophenotypic characteristics of tumor cells forming cancer cell nests within extratumoral lymphatics. Based on the morphological analysis, we postulated that tumor cells forming "Type B" clusters may exhibit a metastatic preference for the lung parenchyma via a lymphatic route. To examine the biological characteristics of these tumor cells, we compared the immunophenotypes of the tumor cells forming "Type A" and "Type B" clusters (Fig. 2). Twenty cases from each of the "Type A" and "Type B" groups were selected. Although their clinicopathological characteristics are not shown, the only significant difference between the two groups was in the number of PM. The staining scores are summarized in Table 4.

Table 3. Clinicopathological characteristics of patients exhibiting extratumoral lymphatic permeation, with or without intrapulmonary metastasis

	Ly^{ext}(+) and PM(−) (n = 90)	Ly^{ext}(+) and PM(+) (n = 47)	P-value
Gender			
Men (n)	62	30	0.57
Women (n)	28	17	
Age range (years)	41–82	44–84	0.06
Median age (years)	65	67	
Smoking habit			
Never smoked (n)	27	18	0.34
Ex or current smoker (n)	63	29	
Carcinoembryonic antigen (ng/mL)			
≤5 (n)	49	22	0.47
>5 (n)	41	25	
Tumor size (cm)	1.0–16	1.3–12	
Median size (cm)	2.9	3.5	0.15
N status			
pN0 (n)	18	8	0.82
pN1–2 (n)	72	39	
Pleural invasion			
No (n)	37	16	0.46
Yes (n)	53	31	
Vascular invasion			
No (n)	24	8	0.29
Yes (n)	66	39	
Morphologic pattern of intralymphatic tumor cells			
Type A (n)	43	11	0.006
Type B (n)	47	36	

Ly^{ext}, extratumoral lymphatic permeation; PM, intrapulmonary metastasis.

Cell proliferation and anoikis resistance markers. The mean (±SE) positive ratio for Geminin in the Type A and Type B groups was 20.3 ± 2.6% and 11.9 ± 2.5%, respectively. Mean (±SE) staining scores in the Type A and Type B groups were 7.8 ± 3.3% and 2.4 ± 0.5%, respectively, for cleaved caspase 3 and 33.5 ± 9.9 and 22.5 ± 6.2, respectively, for p-Src. The expression of Geminin and cleaved caspase 3 was significantly lower in the Type B group than in the Type A group (P = 0.008 and P = 0.01, respectively), but there was no significant difference in p-Src expression between the two groups (P = 0.78).

Adhesion-related molecules. The mean (±SE) staining scores in the Type A and Type B groups were 20.5 ± 9.6 and 43.0 ± 10.4, respectively, for CD44; 31.5 ± 6.9 and 60.5 ± 9.3, respectively, for E-cadherin; and 18.5 ± 6.5 and 9.5 ± 3.6, respectively, for fibronectin. The expression of CD44 and E-cadherin was significantly higher in the Type B than Type A group (P = 0.04 and P = 0.02, respectively), but there was no significant difference in fibronectin levels between the two groups (P = 0.50).

Growth factor receptors. The mean (±SE) staining scores in the Type A and Type B groups were 9.0 ± 5.4 and 25.5 ± 9.0, respectively, for EGFR; 72.5 ± 11.5 and 92.0 ± 13.3, respectively, for IGFR; and 49.8 ± 5.4 and 47.3 ± 10.3, respectively, for c-Met. The expression of EGFR was significantly higher in the Type B than Type A group, but there were no significant differences in the expression of IGFR or c-Met between the two groups (P = 0.29 and P = 0.86, respectively).

Stromal cells around the cancer nest. The mean (±SE) number of cells in the Type A and Type B groups was 4.6 ± 1.4 and 9.5 ± 1.0, respectively, for infiltrating CD204-positive macrophages; 3.8 ± 3.4 and 8.7 ± 7.5, respectively, for CD3-positive T lymphocytes; and 1.3 ± 1.7 and 0.2 ± 0.2, respectively, for CD79a-positive B lymphocytes. No significant differences were observed between the two groups in the expression of CD3 and CD79a (P = 0.14 and P = 0.72, respectively), but the expression of CD204 was significantly higher in the Type B group than in the Type A group (P = 0.007).

Others. The mean (±SE) staining score for CA-IX, a marker of hypoxia, in the Type A and Type B groups was 17.0 ± 4.0 and 16.5 ± 4.7, respectively. There was no significant difference in CA-IX expression between the two groups.

Immunophenotypic characteristics of tumor cells among the primary tumors. In the same 40 cases described above, we also evaluated the immunophenotypes of the tumor cells among the primary tumors. (Note, the staining scores are not shown.) In this examination, only the expression of cleaved caspase 3

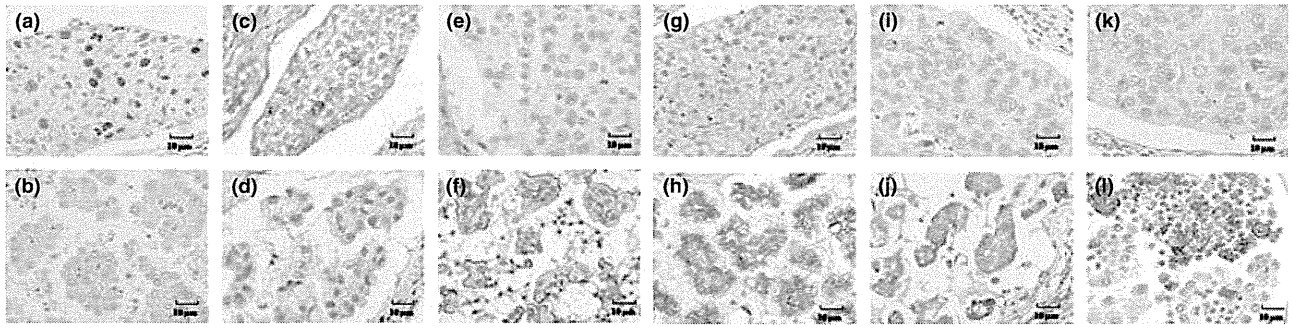

Fig. 2. Immunohistochemical staining of (a,c,e,g,i,k) Type A and (b,d,f,h,j,l) Type B tumor cell nests within permeated lymphatic vessels. (a,b) Geminin, (c,d) cleaved caspase-3, (e,f) CD44, (g,h) E-cadherin, (i,j) epidermal growth factor receptor, and (k,l) CD204.

Table 4. Immunohistochemical staining scores of tumors in lymphatic vessels

Antibodies and their purpose	Type A dominant (n = 20)	Type B dominant (n = 20)	P-value
Proliferation and anoikis resistance			
Geminin	**20.3 ± 2.6**	**11.9 ± 2.5**	**0.008**
Cleaved caspase 3	**7.8 ± 3.3**	**2.4 ± 0.5**	**0.01**
p-Src	33.5 ± 9.9	22.5 ± 6.2	0.78
Adhesion-related molecules			
CD44	**20.5 ± 9.6**	**43.0 ± 10.4**	**0.04**
E-Cadherin	31.5 ± 6.9	60.5 ± 9.3	0.02
Fibronectin	18.5 ± 6.5	9.5 ± 3.6	0.50
Laminin-5γ3	21.5 ± 6.7	29.7 ± 9.0	0.47
Growth factor receptors			
EGFR	**9.0 ± 5.4**	**25.5 ± 9.0**	**0.04**
IGFR	72.5 ± 11.5	92 ± 13.3	0.29
c-Met	49.8 ± 9.4	47.3 ± 10.3	0.86
Stromal cells			
CD3	3.8 ± 3.4	8.7 ± 7.5	0.14
CD79a	1.3 ± 1.7	0.2 ± 0.2	0.72
CD204	**4.6 ± 1.4**	**9.5 ± 2.0**	**0.007**
Others			
CA-IX	17.0 ± 4.0	16.5 ± 4.7	0.78

Data are the mean ± SD. Bolded typeface indicates significant differences. EGFR, epidermal growth factor receptor; IGFR, insulin-like growth factor receptor; CA-IX, carbonic anhydrase IX.

differed significantly between the two groups, being lower in the Type B than Type A group.

Discussion

During the early phase of metastatic tumor development, floating cancer cells proliferate within the vessel lumen, adhere to the endothelium, extravasate from the vessel lumen, migrate into the connective tissue surrounding the vessels, and invade the target organ parenchyma. During each of these processes, cancer cells, accompanied by the surrounding stromal cells, organize their peculiar microenvironment. The present study is the first to show that pulmonary metastasis is correlated with the morphologic and immunophenotypic characteristics of intralymphatic cancer cells and infiltrating stromal cells.

E-Cadherin is now regarded as a key marker for EMT. In the field of carcinogenesis, EMT has been recognized as a phenomenon during which tumor cells in primary lesions invade the surrounding stroma, repressing the transcription of the adherens junction protein E-cadherin.[9–11] Recently, many studies have postulated that the loss or repression of E-cadherin is strongly linked with cancer invasiveness, metastasis, and patient prognosis.[9,12] In contrast with these reports on the repression of E-cadherin and tumor invasiveness, the expression E-cadherin in the present study was elevated in the Type B group, even though this group exhibited more PM than the Type A group. Wells *et al.*[11] discussed the role of E-cadherin in the cancer-associated mesenchymal-epithelial reverting transition (MErT) at distant metastatic sites and speculated that micrometastases may undergo a transition to become E-cadherin positive, just as the critical EMT event is the downregulation or silencing of E-cadherin. Others[13,14] have also reported that the expression of E-cadherin at the metastatic site is higher than that at the primary site, consistent with the results of the present study.

Epithelial growth factor receptor is a receptor tyrosine kinase that plays essential roles under both normal physiological and cancerous conditions. Ligand binding to the EGFR leads to epithelial cell migration away from cohesive masses secondary to E-cadherin downregulation.[11] Some studies[15,16] have reported that inhibition of the autocrine EGFR loop results in E cadherin re-expression and cell–cell cohesion. These reports are in contrast with our results, in which the expression of EGFR was higher in the Type B group than in the Type A group, although the expression of E-cadherin was also higher in the Type B group. These findings suggest that these morphologic and immunophenotypic differences in the tumor cells within lymphatic vessels are not associated with EMT.

CD44 is an integral membrane glycoprotein that functions as a receptor for the extracellular matrix glycan hyaluronan. The expression of CD44 in the Type B group was higher than that in the Type A group, similar to the results for E-cadherin. These findings indicate that an adhesive ability may be deeply associated with the intrapulmonary metastatic process. Some studies[17–20] have also reported that the expression of CD44 is associated with cancer metastasis. Tomlinson *et al.*[21] examined cell lines and human cancers and reported that, as a result of homophilic and homodimeric interactions among E-cadherin, the E-cadherin/α,β-catenin axis-associated adhesive network mediates tumor cell–tumor cell aggregates that are characteristic of the lymphovascular emboli observed during lymphovascular invasion.

The lower expression of Geminin and cleaved caspase 3 in the Type B group indicates that lower proliferative and apoptotic activities are present in this group. In a review, Wells *et al.*[11] reported that metastatic seed cancer cells may inertly become part of the ectopic tissue and therefore surmount the metastatic inefficiencies to which most disseminated cancer cells succumb. Many other studies have also suggested that tumor cells with metastatic potential have a repressed proliferative activity and the ability to resist apoptosis,[3,10,22] also known as anoikis.

The tyrosine kinase Src is one of the key molecules that play a critical role in the development of resistance to apoptosis, known as anoikis.[23,24] However, in present study no significant differences in the expression of p-Src were observed between the Type A and Type B groups. This result does not coincide with the results for cleaved caspase 3, which indicated a lower level of apoptosis in the Type B group. The environment within the lymphatic vessels was inappropriate for tumor cells, so the anoikis resistance process via p-Src may be fully activated in both the Type A and Type B groups. Thus, another mechanism underlying apoptotic resistance within lymphatic vessels may exist.

Regarding stromal cells around cancer nests, Ohtaki *et al.*[25] recently suggested that CD204-positive macrophages clearly reflect the tumor-promoting phenotype of tumor-associated macrophages in lung adenocarcinoma. In the present study, the number of infiltrating CD204-positive macrophages around and within the cancer nests was significantly higher in the Type B group than in the Type A group. This implies that not only tumor cells, but also stromal cells (such as CD204-positive macrophages) may contribute to changing the intralymphatic microenvironment. Zhang *et al.*[26] also advocated that the intravascular microenvironment is a critical staging area for the development of metastases that subsequently invade the parenchyma.

We hypothesized that there may be hypoxic area in the center of the Type A cluster, so we performed CA-IX immunostaining, However, there were no significant differences in CA-IX staining scores between the Type A and Type B groups.

Conversely, in the primary tumors, no significant differences were observed in immunohistochemical staining scores between Type A and Type B groups, except for that of cleaved caspase 3. These differences in staining scores between the

doi: 10.1111/j.1349-7006.2012.02275.x

intralymphatic cancer nests and primary tumors may be explained by the possibility that primary tumors are composed of a strongly heterogeneous cell population phenotypically and functionally. Conversely, intralymphatic tumors may be comprised of a relatively less heterogeneous cell population. Alternatively, cancer cells that have already permeated into lymphatic vessels perceive signals from circulating stromal cells, which lead to phenotypic changes to the cancer cells. However, we could not find any apparent differences in lymphatic vessel morphology and characteristics between Type A and Type B groups in the present study.

In conclusion, the present study clearly shows an association between the morphological and immunophenotypic features of tumor cells and stromal cells within lymphatics and pulmonary metastasis. From this finding, metastasis is predicted to proceed through dynamic changes in the intralymphatic microenvironment, demonstrating that the lymphatic vessels are far from merely a conduit connecting the primary site with the metastatic site. A more mechanistically oriented experimental approach is required to elucidate the key regulator(s) of the intralymphatic microenvironment, possibly leading to useful therapeutic options in the years to come.

Acknowledgments

The authors thank Shinya Yanagi for technical support. This work was supported by a Grant-in-Aid for Cancer Research (19–10) from the Ministry of Health, Labour, and Welfare Programs; the Foundation for the Promotion of Cancer Research, 3rd-Term Comprehensive 10-Year Strategy for Cancer Control; Program for Promotion of Fundamental Studies in Health Sciences of the National Institute of Biomedical Innovation; and JSPS KAKENHI (20590417).

Disclosure

All work reported herein was performed at the National Cancer Center Hospital East, Kashiwa, Chiba, Japan. The research was approved by the Internal Review Board of the institution. No patient consent was required as the research is a retrospective chart review and no personally identifiable information was included in the manuscript. The authors have no conflict of interest to disclose.

References

1 Aokage K, Ishii G, Ohtaki Y *et al.* Dynamic molecular changes associated with epithelial–mesenchymal transition and subsequent mesenchymal–epithelial transition in the early phase of metastatic tumor formation. *Int J Cancer* 2010; **128**: 1585–95.
2 Saijo T, Ishii G, Ochiai A *et al.* Evaluation of extratumoral lymphatic permeation in non-small cell lung cancer as a means of predicting outcome. *Lung Cancer* 2007; **55**: 61–6.
3 Sakuma Y, Takeuchi T, Nakamura Y *et al.* Lung adenocarcinoma cells floating in lymphatic vessels resist anoikis by expressing phosphorylated Src. *J Pathol* 2010; **220**: 574–85.
4 Ishii G, Ito TK, Aoyagi K *et al.* Presence of human circulating progenitor cells for cancer stromal fibroblasts in the blood of lung cancer patients. *Stem Cells* 2007; **25**: 1469–77.
5 Duda DG, Duyverman AM, Kohno M *et al.* Malignant cells facilitate lung metastasis by bringing their own soil. *Proc Natl Acad Sci USA* 2010; **107**: 21677–82.
6 Girard N, Deshpande C, Lau C *et al.* Comprehensive histologic assessment helps to differentiate multiple lung primary nonsmall cell carcinomas from metastases. *Am J Surg Pathol* 2009; **33**: 1752–64.
7 Union for International Cancer Control (UICC). *TNM Classification of Malignant Tumours*, 6th edn. Geneva: UICC, 2002.
8 Travis W, Coblby T, Corrin B, Shimosato Y, Brambilla E. *Pathology and Genetics of Tumours of the Lung, Pleura, Thymus and Heart*, 3rd edn. Berlin: Springer Verlag, 1999.
9 Onder TT, Gupta PB, Mani SA, Yang J, Lander ES, Weinberg RA. Loss of E-cadherin promotes metastasis via multiple downstream transcriptional pathways. *Cancer Res* 2008; **68**: 3645–54.
10 Thiery JP. Epithelial–mesenchymal transitions in tumour progression. *Nat Rev Cancer* 2002; **2**: 442–54.
11 Wells A, Yates C, Shepard CR. E-Cadherin as an indicator of mesenchymal to epithelial reverting transitions during the metastatic seeding of disseminated carcinomas. *Clin Exp Metastasis* 2008; **25**: 621–8.
12 Ono K, Sugio K, Uramoto H *et al.* Discrimination of multiple primary lung cancers from intrapulmonary metastasis based on the expression of four cancer-related proteins. *Cancer* 2009; **115**: 3489–500.
13 Imai T, Horiuchi A, Shiozawa T *et al.* Elevated expression of E-cadherin and alpha-, beta-, and gamma-catenins in metastatic lesions compared with primary epithelial ovarian carcinomas. *Hum Pathol* 2004; **35**: 1469–76.
14 Kowalski PJ, Rubin MA, Kleer CG. E-Cadherin expression in primary carcinomas of the breast and its distant metastases. *Breast Cancer Res* 2003; **5**: R217–22.
15 Yates CC, Shepard CR, Stolz DB, Wells A. Co-culturing human prostate carcinoma cells with hepatocytes leads to increased expression of E-cadherin. *Br J Cancer* 2007; **96**: 1246–52.
16 Mamoune A, Kassis J, Kharait S *et al.* DU145 human prostate carcinoma invasiveness is modulated by urokinase receptor (uPAR) downstream of epidermal growth factor receptor (EGFR) signaling. *Exp Cell Res* 2004; **299**: 91–100.
17 Kargi HA, Kuyucuoglu MF, Alakavuklar M, Akpinar O, Erk S. CD44 expression in metastatic and non-metastatic non-small cell lung cancers. *Cancer Lett* 1997; **119**: 27–30.
18 Sheridan C, Kishimoto H, Fuchs RK *et al.* CD44 + /CD24− breast cancer cells exhibit enhanced invasive properties: an early step necessary for metastasis. *Breast Cancer Res* 2006; **8**: R59.
19 Singleton PA, Salgia R, Moreno-Vinasco L *et al.* CD44 regulates hepatocyte growth factor-mediated vascular integrity. Role of c-Met, Tiam1/Rac1, dynamin 2, and cortactin. *J Biol Chem* 2007; **282**: 30643–57.
20 Valentiner U, Valentiner FU, Schumacher U. Expression of CD44 is associated with a metastatic pattern of human neuroblastoma cells in a SCID mouse xenograft model. *Tumour Biol* 2008; **29**: 152–60.
21 Tomlinson JS, Alpaugh ML, Barsky SH. An intact overexpressed E-cadherin/alpha,beta-catenin axis characterizes the lymphovascular emboli of inflammatory breast carcinoma. *Cancer Res* 2001; **61**: 5231–41.
22 Al-Mehdi AB, Tozawa K, Fisher AB, Shientag L, Lee A, Muschel RJ. Intravascular origin of metastasis from the proliferation of endothelium-attached tumor cells: a new model for metastasis. *Nat Med* 2000; **6**: 100–2.
23 Wei L, Yang Y, Zhang X, Yu Q. Altered regulation of Src upon cell detachment protects human lung adenocarcinoma cells from anoikis. *Oncogene* 2004; **23**: 9052–61.
24 Windham TC, Parikh NU, Siwak DR *et al.* Src activation regulates anoikis in human colon tumor cell lines. *Oncogene* 2002; **21**: 7797–807.
25 Ohtaki Y, Ishii G, Nagai K *et al.* Stromal macrophage expressing CD204 is associated with tumor aggressiveness in lung adenocarcinoma. *J Thorac Oncol* 2010; **10**: 1507–15.
26 Zhang Q, Yang M, Shen J, Gerhold LM, Hoffman RM, Xing HR. The role of the intravascular microenvironment in spontaneous metastasis development. *Int J Cancer* 2010; **126**: 2534–41.

Supporting Information

Additional Supporting Information may be found in the online version of this article:

Fig. S1. The rate of Type A and Type B cancer cell nests in patients with extratumoral lymphatic permeation.

Please note: Wiley-Blackwell are not responsible for the content or functionality of any supporting materials supplied by the authors. Any queries (other than missing material) should be directed to the corresponding author for the article.

Influence of Cigarette Smoking on Survival and Tumor Invasiveness in Clinical Stage IA Lung Adenocarcinoma

Ryo Maeda, MD, Junji Yoshida, MD, Genichiro Ishii, MD, Tomoyuki Hishida, MD, Mitsuyo Nishimura, MD, and Kanji Nagai, MD

Departments of Thoracic Oncology and Pathology, National Cancer Center Hospital East, Kashiwa, Chiba, Japan

Background. The objective of this study was to investigate the association between cigarette smoking, cancer survival, and pathological features of clinical stage IA lung adenocarcinoma.

Methods. Between August 1992 and December 2007, 1,070 consecutive patients with clinical stage IA lung adenocarcinoma underwent complete resection with systematic lymph node dissection. Univariate analysis by log-rank tests was performed to determine unfavorable prognostic factors, and the Cox proportional hazards regression model was used to identify the potential independent predictors.

Results. The overall 5-year survival rate of patients with greater than 20 pack-years (PY > 20) was 71%, significantly lower than patients with 20 or less pack-years (PY ≤ 20; 86%; $p < 0.001$). Postoperative pathological prognostic factors, including moderate or poor histologic differentiation, lymphatic permeation, intratumoral vascular invasion, visceral pleural invasion, and lymph node metastasis, were detected more often in patients with greater than 20 PY. Sixty-five percent of the patients in this study had pathological stage IA tumors, and their overall 5-year survival rates with 20 or less PY and greater than 20 PY were 97% and 86%, respectively ($p < 0.001$).

Conclusions. In patients with clinical stage IA adenocarcinoma, a history of heavy smoking was associated with poor outcomes and was a statistically significant predictor of histologic tumor invasion.

(Ann Thorac Surg 2012;93:1626–32)

Many compounds found in cigarette smoke have been proven to induce lung carcinogenesis [1]. All histologic types of lung cancer are likewise reported to associate significantly with smoking [2–4], with small cell lung cancer and squamous cell carcinoma having the strongest correlation [2]. The most frequently occurring type of lung cancer is adenocarcinoma, which has a rising incidence rate in most countries [3]. A relationship between cigarette smoking and the carcinogenesis of pulmonary adenocarcinoma has been established, although the association is reported to be weak [4, 5].

The correlation between cigarette smoking and postoperative complications is well known [6, 7], but the effect of smoking on lung cancer biology remains unexplored. The objective of this study was to investigate the association between cigarette smoking and pathological characteristics of clinical stage IA lung adenocarcinoma.

Accepted for publication Jan 3, 2012.

Address correspondence to Dr Yoshida, Department of Thoracic Oncology, National Cancer Center Hospital East, 6-5-1, Kashiwanoha, Kashiwa, Chiba, 277-8577, Japan; e-mail: jyoshida@east.ncc.go.jp.

Material and Methods

Patients

Data collection and analyses were approved and the need to obtain written informed consent from each patient was waived by the institutional review board in April 2010. We identified 1,074 consecutive patients with clinical stage IA lung adenocarcinoma from our departmental database at the National Cancer Center Hospital East who underwent complete resection by lobectomy or systematic lymph node dissection between August 1992 and December 2007. Tumor-free gross surgical and histologic margins characterized complete resections. The study excluded 4 patients who received preoperative chemotherapy, radiation therapy, or both, leaving 1,070 subjects.

Pathological Evaluations

Lung cancer histology type was determined by World Health Organization classifications [8]. In situ adenocarcinomas were included in the study. Tumors were histologically graded on their structural and cytologic atypia as either well-, moderately, or poorly differentiated carcinomas by a single pathologist (G.I.) blinded to the clinical outcomes. The histopathological stage of each tumor was postoperatively determined according to TNM classifications from the International Union Against Cancer, 7th edition [9]. Blood vessels were iden-

Published by Elsevier Inc

0003-4975/$36.00
doi:10.1016/j.athoracsur.2012.01.005

tified by hematoxylin-eosin and elastin (Victoria blue-van Gieson) staining, and visceral pleural invasion was evaluated. Intratumoral vascular invasion was diagnosed from histologic examinations that identified cancer cells within the blood vessels.

Clinicopathological Evaluations

Information on cigarette smoking status was prospectively collected from hospital outpatient questionnaires completed by patients at their first clinic visit. Patients were asked to record the age at which they started smoking, duration of smoking, and average number of cigarettes smoked daily. Pack-years (PY) were defined as the number of cigarette packs (20 cigarettes per pack) smoked per day multiplied by years of smoking and used to quantify smoking history. Patients were classified into one of six groups by their smoking history: A (never smoked; PY = 0), B (greater than 0, but less than or equal to 10; $0 < PY \leq 10$), C (greater than 10, but less than or equal to 20; $10 < PY \leq 20$), D (greater than 20, but less than or equal to 40; $20 < PY \leq 40$), E (greater than 40, but less than or equal to 60; $40 < PY \leq 60$), and F (greater than 60; $PY > 60$). Just before surgery, all patients were instructed to cease smoking.

Chest computed tomography was performed during clinical examination of each patient to measure tumor size. Regional lymph node metastasis was clinically defined as a short-axis diameter of greater than 1.0 cm. Integrated positron emission tomography was not performed for clinical stage IA patients in clinical staging.

The medical records for each patient were reviewed to categorize the following information: age (dichotomized at the median age of 65 years), sex, smoking history (groups A, B, C, D, E, or F), tumor diameter measured by preoperative chest computed tomography (dichotomized at 2.0 cm), tumor laterality (right or left), primary lobe (upper/middle lobe or lower lobe), maximal diameter of the resected tumor (dichotomized at 2.0 cm), histologic differentiation (well-, moderately, or poorly differentiated), intratumoral vascular invasion (present or absent), lymphatic permeation (present or absent), visceral pleural invasion (as defined by TNM classification, 7th edition [9]; present or absent), intrapulmonary metastasis (present or absent), and lymph node metastasis (N0 or N1 through N33).

Statistical Analysis

Differences in categorical outcomes were evaluated using the χ^2 test. Overall survival was calculated in months from the date of resection to the date of death from any cause or the last patient follow-up. The recurrence-free period was calculated in months from the date of resection to the date of the first recurrence or last follow-up. For calculation of the recurrence-free proportion, patients who died without recurrence or had no recurrence on the last date of contact were censored. Cumulative survival rates and recurrence-free proportions were estimated using the Kaplan-Meier method, and differences in variables were evaluated using the log-rank test. Multivariate Cox proportional hazards models were used to identify independent predictors. All statistical tests were two-sided, with the level of significance set at a probability value of less than 0.05. All analyses were performed with the statistical software SPSS 11.0 (Dr. SPSS II for Windows, standard version 11.0, SPSS Inc, Chicago, IL).

Results

Clinical Prognostic Factors

Median follow-up period after surgical resection was 57 months (range, 1 to 152 months), and the overall 5-year survival rate of the 1,070 patients was 80.3%. Overall survival curves of patients arranged by smoking history are displayed in Figure 1A. Overall 5-year survival rates of patients in groups A (PY = 0), B ($0 < PY \leq 10$), C ($10 < PY \leq 20$), D ($20 < PY \leq 40$), E ($40 < PY \leq 60$), and F ($PY >$

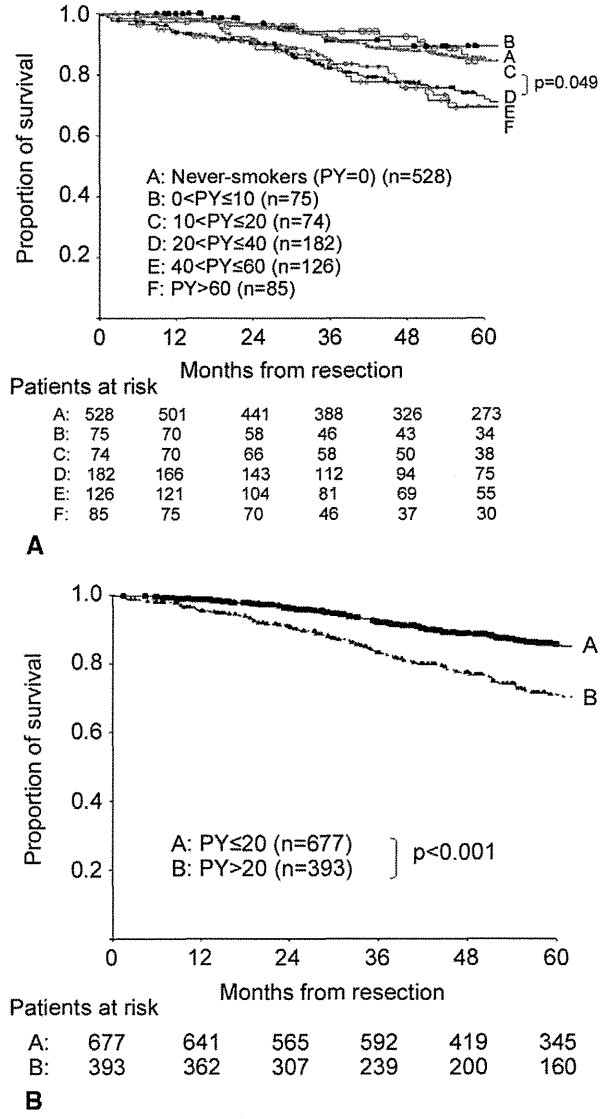

Fig 1. (A) Overall survival curves according to smoking history in entire cohort. (B) Overall survival curves of patients with 20 or less pack-years (PY) smoking history and greater than 20 pack-years smoking history.